

Single-hole Green's functions in insulating copper oxides at nonzero temperature

J. van den Brink* and O. P. Sushkov†

School of Physics, The University of New South Wales, Sydney 2052, Australia

(Received 4 August 1997)

We consider the single-hole dynamics in a modified t - J model at finite temperature. The modified model includes a next-nearest (t') and next-next-nearest (t'') hopping. The model has been considered before in the zero temperature limit to explain angle-resolved photoemission measurements. We extend this consideration to the case of finite temperature where long-range antiferromagnetic order is destroyed, using the self-consistent Born approximation. The Dyson equation which relates the single-hole Green's functions for a fixed pseudospin and for fixed spin is derived. The Green's function with fixed pseudospin is infrared stable but the Green's function with fixed spin is close to an infrared divergence. We demonstrate how to renormalize this Green's function in order to assure numerical convergence. At nonzero temperature the quasiparticle peaks shift to lower energy and are broadened. The temperature broadening is, however, not enough to explain the widths of the experimental data, indicating that other degrees of freedom contribute to the quasiparticle damping.[S0163-1829(98)03205-6]

I. INTRODUCTION

Recent angle-resolved photoemission spectroscopy (ARPES) measurements by Wells *et al.*¹ and by Pothuizen *et al.*² on the insulating copper oxide $\text{Sr}_2\text{CuO}_2\text{Cl}_2$ provide a unique experimental probe of the properties of a single hole in an antiferromagnetic background. Theoretically this problem was analyzed in terms of a t - t' - J model using exact diagonalization techniques for small clusters⁴ and the self-consistent Born approximation (SCBA).⁵ From a recent evaluation of the hopping integrals it was concluded that the next-next-nearest-neighbor hopping matrix element t'' is significant and almost as large as the diagonal hopping matrix element t' , so that t'' should also be incorporated in a model Hamiltonian.⁶ This was done in a recent paper,⁷ where also the leading corrections to the SCBA were evaluated.

The ARPES experiments¹⁻³ are carried out at a temperature of 300–350 K, which is above the Néel temperature of this compound. Theoretical treatments up to now, however, restrict themselves to the zero-temperature limit, assuming long-range antiferromagnetic order, and spectra are artificially broadened in order to compare with experiment. It is therefore important to extend the SCBA calculations to finite temperature, where long-range antiferromagnetic order is lacking, although at room temperature the magnetic correlation length for this compound is still about 60 lattice spacings and no drastic deviation of the ARPES spectrum at room temperature from the one at zero temperature is expected. Another motivation for this work is that a SCBA technique that can cope with the absence of long-range magnetic order may be extended in the future to describe the quantum-disordered state of the doped copper oxides.

We consider a two-dimensional (2D) t - t' - t'' - J model at finite temperature. We apply the modified spin-wave theory suggested by Takahashi for 2D Heisenberg model at nonzero temperature⁸ to deal with a state without long-range antiferromagnetic order. The Hamiltonian for the t - t' - t'' - J model is

$$H = -t \sum_{\langle ij \rangle \sigma} c_{i\sigma}^\dagger c_{j\sigma} - t' \sum_{\langle ij_1 \rangle \sigma} c_{i\sigma}^\dagger c_{j_1\sigma} - t'' \sum_{\langle ij_2 \rangle \sigma} c_{i\sigma}^\dagger c_{j_2\sigma} + J \sum_{\langle ij \rangle \sigma} \mathbf{S}_i \cdot \mathbf{S}_j, \quad (1)$$

where $c_{i\sigma}^\dagger$ is the creation operator of an electron with spin σ ($\sigma = \uparrow, \downarrow$) at site i on the two-dimensional square lattice, $\langle ij \rangle$ represents nearest-neighbor sites, $\langle ij_1 \rangle$ next-nearest-neighbor sites (diagonal), and $\langle ij_2 \rangle$ represents next-next-nearest sites. The spin operator is $\mathbf{S}_i = \frac{1}{2} c_{i\alpha}^\dagger \boldsymbol{\sigma}_{\alpha\beta} c_{i\beta}$. The exchange derived from two-magnon Raman scattering is $J = 125$ meV.^{9,10} Following the most recent calculation of the hopping matrix elements performed by Andersen *et al.*⁶ we take $t = 386$ meV, $t' = -105$ meV, and $t'' = 86$ meV. We set $J = 1$, so that in these units

$$t = 3.1, \quad t' = -0.8, \quad t'' = 0.7. \quad (2)$$

We first calculate the hole Green's function with fixed pseudospin at finite temperature, introduced by a constraint on the sublattice magnetization, and evaluate the contribution to the self-energy due to the virtual emission and absorption of spin waves by the hole. Then the hole Green's function with fixed spin, which corresponds to a Green's function that is actually measured in ARPES, is calculated. This Green's function turns out to be close to an infrared divergence and we show that this instability can be avoided by a proper renormalization, assuring that the results numerically converge even when a rather limited number of grid points is used. We find that at nonzero temperature the quasiparticle peaks broaden and shift to lower energy. The shift is independent of momentum and is due to the larger effective hole bandwidth as at finite temperature the spin order is frustrated.

II. HOLE GREEN'S FUNCTION WITH FIXED PSEUDOSPIN G_D

At half filling (one electron per site) the model under consideration is equivalent to a Heisenberg model. We are

interested in the situation when one electron is removed from the system, and so when a single hole is produced. The dynamics of a single hole in an antiferromagnetic background can be described by the SCBA.^{11,12} This approximation works very well due to the absence of single-loop corrections to the hole–spin-wave vertex.^{13–15} Now we have to modify the SCBA for finite temperature. The main complication is that at finite temperature there is no long-range antiferromagnetic order. Nevertheless, following Takahashi⁸ we introduce artificially two sublattices: up and down. The bare hole operator d_i is defined so that $d_i^\dagger \propto c_{i\uparrow}$ on the \uparrow sublattice and $\propto c_{i\downarrow}$ on the \downarrow sublattice. In momentum representation,

$$\begin{aligned} d_{\mathbf{k}\downarrow}^\dagger &= \sqrt{\frac{2}{N(1/2+m)}} \sum_{i \in \downarrow} c_{i\downarrow} e^{i\mathbf{k} \cdot \mathbf{r}_i}, \\ d_{\mathbf{k}\uparrow}^\dagger &= \sqrt{\frac{2}{N(1/2+m)}} \sum_{j \in \uparrow} c_{j\uparrow} e^{i\mathbf{k} \cdot \mathbf{r}_j}, \end{aligned} \quad (3)$$

where N is the number of sites and $m = \langle S_{iz} \rangle = 0$ is the average magnetization. The brackets $\langle \rangle$ denote both quantum and statistical averaging. The quasimomentum \mathbf{k} is restricted to be inside the magnetic Brillouin zone: $\gamma_{\mathbf{k}} = \frac{1}{2}(\cos k_x + \cos k_y) \geq 0$. In this notation it looks like $d_{\mathbf{k}\sigma}$ has spin $\sigma = \pm 1/2$, but actually rotation invariance is violated and σ is a pseudospin which just labels the two sublattices. Nevertheless, the pseudospin gives the correct value of the spin- z projection: $S_z = \sigma = \pm 1/2$. The coefficients in Eqs. (3) provide the correct normalization:

$$\langle d_{\mathbf{k}\downarrow} d_{\mathbf{k}\downarrow}^\dagger \rangle = \frac{4}{N} \sum_{i \in \downarrow} \langle c_{i\downarrow}^\dagger c_{i\downarrow} \rangle = 2 \left(\frac{1}{2} + \langle S_{iz} \rangle \right) = 1. \quad (4)$$

The retarded hole Green's function is defined as

$$G_d(\boldsymbol{\epsilon}, \mathbf{k}) = -i \int_0^\infty \langle d_{\mathbf{k}\sigma}(\tau) d_{\mathbf{k}\sigma}^\dagger(0) \rangle e^{i\boldsymbol{\epsilon}\tau} d\tau. \quad (5)$$

The t', t'' terms in the Hamiltonian (1) correspond to the hole hopping inside one sublattice. This gives the bare hole dispersion

$$\begin{aligned} \epsilon_{0\mathbf{k}} &= 4t' \cos k_x \cos k_y + 2t''(\cos 2k_x + \cos 2k_y) \\ &\rightarrow \beta_{01} \gamma_{\mathbf{k}}^2 + \beta_{02} (\gamma_{\mathbf{k}}^-)^2, \end{aligned} \quad (6)$$

where $\gamma_{\mathbf{k}}^- = \frac{1}{2}(\cos k_x - \cos k_y)$, $\beta_{01} = 4(2t'' + t')$, and $\beta_{02} = 4(2t'' - t')$. In Eq. (6) we took into account that the sign of a hole dispersion is opposite to that for an electron (the maximum of the electron band corresponds to the minimum of the hole band), and omitted the constant term. The bare hole Green's function is

$$G_{0d}(\boldsymbol{\epsilon}, \mathbf{k}) = \frac{1}{\boldsymbol{\epsilon} - \epsilon_{0\mathbf{k}} + i0}. \quad (7)$$

For spin excitations we use the modified spin-wave theory⁸ (see also the review paper in Ref. 16). In order to treat the Heisenberg term in the Hamiltonian (1) within spin-wave theory, it is convenient to use the Dyson-Maleev transformation¹⁷ for a localized spin $S = 1/2$,

$$S_l^- = a_l^\dagger, \quad S_l^+ = (2S - a_l^\dagger a_l) a_l, \quad S_l^z = S - a_l^\dagger a_l$$

for $l \in$ up sublattice,

$$S_m^- = b_m, \quad S_m^+ = b_m^\dagger (2S - b_m^\dagger b_m), \quad S_m^z = -S + b_m^\dagger b_m$$

for $m \in$ down sublattice,

(8)

and the Fourier representation for a_l and b_m :

$$a_l = \sqrt{\frac{2}{N}} \sum_{\mathbf{q}} e^{i\mathbf{q} \cdot \mathbf{r}_l} a_{\mathbf{q}}, \quad b_m = \sqrt{\frac{2}{N}} \sum_{\mathbf{q}} e^{i\mathbf{q} \cdot \mathbf{r}_m} b_{\mathbf{q}}. \quad (9)$$

The summation over \mathbf{q} , here and everywhere below, is restricted inside the magnetic Brillouin zone. There are essentially two ways to find an effective Hamiltonian quadratic in the operators a and b . The first way is to just drop the quartic terms as is done in linear spin-wave theory (LSWT). The second way is to treat the quartic terms at the mean-field level $a^\dagger a b^\dagger b \rightarrow \langle a^\dagger a \rangle b^\dagger b + \langle a^\dagger b^\dagger \rangle a b + \dots$, corresponding to mean-field spin-wave theory. As both approximations give very close results we choose to use LSWT because it is simpler in the present context.

A. Finite-temperature correction for G_d

So far we followed the zero-temperature derivation for the SCBA. We take the approach of calculating the finite-temperature corrections to the hole Green's function G_d with a diagrammatic, perturbative, method. This framework can be used if the number of spin waves per site is small, i.e., if T/J is not too large. This is a reasonable prerequisite as in the experiments T/J is of the order of 1/4. We will show later on that at these temperatures the number of spin waves is actually small, justifying our approach. The advantage of this approach over performing the calculations at imaginary, Matsubara, frequencies is that in our framework the absence of long-range antiferromagnetic order is specifically built in. Problems with the numerical analytic continuation on the real frequency axis are avoided. As is shown later on, an almost divergency occurs that demands large lattices in order to get stable results. By performing the calculation on the real axis from the beginning, the Green's function can be renormalized, lifting the almost divergency.

At nonzero temperatures the long-range antiferromagnetic order is destroyed. Very many long-wavelength spin waves are excited, and one must take into account their nonlinear interaction. An approximate way to do it is to impose an additional condition that sublattice magnetization be zero,⁸

$$\langle S_{l \in \uparrow}^z - S_{m \in \downarrow}^z \rangle = \langle \frac{1}{2} - a_l^\dagger a_l + \frac{1}{2} - b_m^\dagger b_m \rangle = 0. \quad (10)$$

This constraint gives an effective cutoff of unphysical states in the Dyson-Maleev transformation. The constraint (10) is introduced into the Hamiltonian via a Lagrange multiplier $\frac{1}{8} \nu^2$. Now we must diagonalize

$$H_{\text{eff}} = H_{\text{LSWT}} - \frac{1}{8} \nu^2 (S_{l \in \uparrow}^z - S_{m \in \downarrow}^z) \rightarrow 2 \sum_{\mathbf{q}} [A(a_{\mathbf{q}}^\dagger a_{\mathbf{q}} + b_{\mathbf{q}}^\dagger b_{\mathbf{q}}) + \gamma_{\mathbf{q}}(a_{\mathbf{q}} b_{-\mathbf{q}} + a_{\mathbf{q}}^\dagger b_{-\mathbf{q}}^\dagger)], \quad (11)$$

where $A = 1 + \nu^2/8$. This can be done by the Bogoliubov transformation

$$a_{\mathbf{q}} = u_{\mathbf{q}} \alpha_{\mathbf{q}} + v_{\mathbf{q}} \beta_{-\mathbf{q}}^\dagger, \quad b_{-\mathbf{q}} = v_{\mathbf{q}} \alpha_{\mathbf{q}}^\dagger + u_{\mathbf{q}} \beta_{-\mathbf{q}}, \quad (12)$$

and we find the effective spectrum and Bogoliubov parameters

$$\omega_{\nu\mathbf{q}} = 2\sqrt{A^2 - \gamma_{\mathbf{q}}^2}, \quad u_{\mathbf{q}} = \sqrt{\frac{A}{\omega_{\nu\mathbf{q}}} + \frac{1}{2}},$$

$$v_{\mathbf{q}} = -\text{sgn}(\gamma_{\mathbf{q}}) \sqrt{\frac{A}{\omega_{\nu\mathbf{q}}} - \frac{1}{2}}. \quad (13)$$

These equations show that at nonzero temperature the spin-wave spectrum has a gap $\nu\sqrt{1 + \nu^2/16} \approx \nu$. This elucidates the meaning of the constraint and the Lagrange multiplier. Taking into account that in thermal equilibrium

$$n_{\mathbf{q}} \equiv \langle \alpha_{\mathbf{q}}^\dagger \alpha_{\mathbf{q}} \rangle = \langle \beta_{\mathbf{q}}^\dagger \beta_{\mathbf{q}} \rangle = \frac{1}{\exp(\omega_{\nu\mathbf{q}}/T) - 1}, \quad (14)$$

we obtain from Eq. (10) the equation for ν ,

$$0 = 1 - \frac{2}{N} \sum_{\mathbf{q}} \frac{A}{\omega_{\nu\mathbf{q}}} (1 + 2n_{\mathbf{q}}). \quad (15)$$

This equation gives an exponentially small ν and, hence, an exponentially large magnetic correlation length $\xi_M \propto 1/\nu$.

Hopping to a nearest neighbor in the Hamiltonian (1) gives an interaction of the hole with spin waves,

$$H_{h,\text{sw}} = \sum_{\mathbf{k},\mathbf{q}} g_{\mathbf{k},\mathbf{q}} (d_{\mathbf{k}+\mathbf{q}}^\dagger d_{\mathbf{k}\uparrow} \alpha_{\mathbf{q}} + d_{\mathbf{k}+\mathbf{q}}^\dagger d_{\mathbf{k}\downarrow} \beta_{\mathbf{q}} + \text{H.c.}). \quad (16)$$

In diagrams we will denote the vertex $g_{\mathbf{k},\mathbf{q}}$ by a dot; see Fig. 3(d). This vertex is given by¹³⁻¹⁵

$$g_{\mathbf{k},\mathbf{q}} \equiv \langle \alpha_{\mathbf{q}} d_{\mathbf{k}\uparrow} | H_t | d_{\mathbf{k}+\mathbf{q}\downarrow}^\dagger \rangle = 4t \sqrt{\frac{2}{N}} (\gamma_{\mathbf{k}} u_{\mathbf{q}} + \gamma_{\mathbf{k}+\mathbf{q}} v_{\mathbf{q}}). \quad (17)$$

We stress that the vertex (17) has the same form as in the case of zero temperature, except for the pseudogap in the Bogoliubov parameters (13). We remind the reader of the fact that at zero temperature $g_{\mathbf{k},\mathbf{q}=0} = 0$ because of the Goldstone theorem. In the present case, due to the pseudogap, $g_{\mathbf{k},\mathbf{q}=0} \neq 0$. This is a reflection of the fact that the long-range antiferromagnetic order is destroyed. However, as the pseudogap is small, its presence will not give rise to large effects in the spectra.

Similar to the zero-temperature case the spin structure of the interaction (16) forbids single-loop corrections to the hole-spin-wave vertex, so that the self-energy is of the form



FIG. 1. Self-energy at finite temperature. The solid line represents the hole Green's function G_d , and the dashed line represents the spin wave. The first diagram corresponds to virtual emission of the spin wave, and the second diagram corresponds to virtual absorption.

$$\Sigma(\epsilon, \mathbf{k}) = \sum_{\mathbf{q}} [(1 + n_{\mathbf{q}}) g_{\mathbf{k}-\mathbf{q},\mathbf{q}}^2 G_d(\epsilon - \omega_{\mathbf{q}}, \mathbf{k} - \mathbf{q}) + n_{\mathbf{q}} g_{\mathbf{k},\mathbf{q}}^2 G_d(\epsilon + \omega_{\mathbf{q}}, \mathbf{k} + \mathbf{q})], \quad (18)$$

where the first term arises from the virtual emission of the spin wave and second term arises from the virtual absorption; see Fig. 1. The self-consistent solution of this equation together with the standard relation

$$G_d(\epsilon, \mathbf{k}) = \frac{1}{\epsilon - \epsilon_{0\mathbf{k}} - \Sigma(\epsilon, \mathbf{k}) + i0} \quad (19)$$

gives the retarded Green's function. Due to the definition of the operators (3), the Green's function (5) is invariant under translation with the inverse vector of the magnetic sublattice $\mathbf{Q} = (\pm\pi, \pm\pi)$,

$$G_d(\epsilon, \mathbf{k} + \mathbf{Q}) = G_d(\epsilon, \mathbf{k}), \quad (20)$$

in spite of the absence of the long-range antiferromagnetic order.

B. Results for G_d

The numerical solution of Eq. (19) is straightforward. To avoid poles we replace $i0 \rightarrow i\Gamma/2 = i0.05$. The energy scale consists of 300 points with variable density (concentrated near sharp structures of G_d). The number of points in the magnetic Brillouin zone is 10^4 which is equivalent to a 140×140 lattice. Actually the results are almost independent of the grid as soon as it is larger than 20×20 . In Fig. 2 the spectral density $-(1/\pi)\text{Im}G_d(\omega, \mathbf{k})$ as a function of ω for a cut through the Brillouin zone from $\mathbf{k} = (\pi/2, \pi/2)$ to $\mathbf{k} = (\pi, 0)$ is shown for two different temperatures.

The number of spin waves per site for the highest temperature, $T = 0.4$, we considered is ≈ 0.05 , and so much

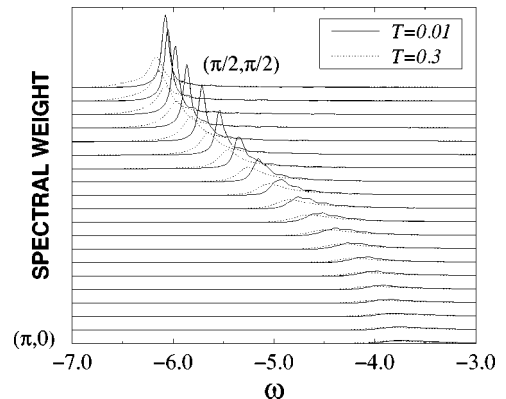


FIG. 2. Plots of $(-1/\pi)\text{Im}G_d(\omega, \mathbf{k})$ as a function of ω for a cut through the Brillouin zone from $\mathbf{k} = (\pi/2, \pi/2)$ to $\mathbf{k} = (\pi, 0)$ for $T = 0.01$ and $T = 0.3$.

smaller than unity, justifying the perturbational approach. We recall that we use the set of parameters (2) based on Ref. 6 and that the same set has been used in Ref. 7 for a zero-temperature calculation. Quasiparticle energies and residues obtained here are quite similar to that at zero temperature.⁷ We see from Fig. 2 that temperature shifts the quasipeaks positions to lower energy and broadens them. The explanation for this is that there are two contributions to the self-energy at nonzero temperatures. One term originates from virtual spin-wave emission processes and the other from virtual spin-wave absorption. The former contribution is also present at $T=0$ and is enhanced at finite temperatures by a factor $1+n_q$; i.e., at finite temperature the interaction between the spin waves and the hole is effectively increased due to this process. The matrix element for the emission of an extra spin wave is larger if the number of spin waves already present is larger, because of the bosonic nature of the spin waves. The part of the self-energy that is due to the spin-wave emission is multiplied by a factor larger than 1 at finite temperature, causing a shift of the quasiparticle peaks to lower energy that is nearly uniform in the Brillouin zone and a shift of the incoherent part of the Green's function to higher energies. This has a simple physical reason. At nonzero temperature the hole propagates more easily because the antiferromagnetic order is frustrated. This causes a uniform shift of all quasiparticle poles to lower energy and does not effect their dispersion, as the quasiparticle dispersion is determined predominantly by the magnetic interaction. So the effect of nonzero temperature is qualitatively different from the effects of doping, where it is found that a reconstruction of the quasiparticle dispersion takes place, attributed to the frustrated magnetic order in the doped system.¹⁸ The contribution to the self-energy at finite temperature due to the spin-wave absorption is mainly responsible for the broadening of the quasiparticle peaks.

III. HOLE GREEN'S FUNCTION WITH FIXED SPIN G_c

The operators $d_{k\uparrow}$ and $d_{k\downarrow}$ discussed in the previous section are defined at different sublattices. The operators on two sublattices are useful as mathematical constructions, but when a photon removes an electron from the system, it does not differentiate between the sublattices, and moreover, at nonzero temperature there are no sublattices at all. Therefore we have to define the particle operator that is relevant for photoemission independent of the sublattice. This particle operator is

$$c_{k\sigma} = \sqrt{\frac{2}{N}} \sum_i c_{i\sigma} e^{ik \cdot r_i}. \quad (21)$$

The normalization is chosen in such a way that

$$\langle 0 | c_{k\uparrow}^\dagger c_{k\uparrow} | 0 \rangle = \frac{2}{N} \langle 0 | \sum_i c_{i\uparrow}^\dagger c_{i\uparrow} | 0 \rangle = 1. \quad (22)$$

The corresponding retarded Green's function is

$$G_c(\epsilon, \mathbf{k}) = -i \int_0^\infty \langle c_{k\sigma}^\dagger(\tau) c_{k\sigma}(0) \rangle e^{i\epsilon\tau} d\tau. \quad (23)$$

This is the Green's function measured in ARPES.

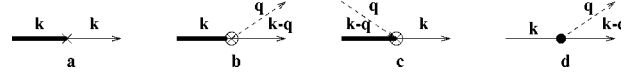


FIG. 3. The vertices (a) single-hole creation, (b) hole+spin-wave creation, (c) hole creation with spin-wave annihilation, and (d) usual hole-spin-wave vertex. The thick line corresponds to G_c , and the thin solid line corresponds to G_d . The dashed line is the spin wave.

Now we have to find the relation between $G_c(\epsilon, \mathbf{k})$ and $G_d(\epsilon, \mathbf{k})$. The operator $c_{k\sigma}$ acting on the half-filled ground state produces a single hole. We denote the corresponding amplitude by $a_{\mathbf{k}}$ and denote it in Fig. 3(a) as a cross. The thick line corresponds to the Green's function G_c and the thin line corresponds to the G_d . The amplitude $a_{\mathbf{k}}$ equals

$$a_{\mathbf{k}} = \langle d_{k\uparrow} c_{k\downarrow} \rangle = \sqrt{\frac{1}{2}}. \quad (24)$$

The operator $c_{k\sigma}$ acting on a state of the system can also produce a hole+spin wave. This amplitude is shown in Fig. 3(b) as a circled cross with the dashed line being a spin wave. We denote this amplitude by $b_{\mathbf{k}, \mathbf{q}}$,

$$\begin{aligned} b_{\mathbf{k}-\mathbf{q}, \mathbf{q}} &= \langle \beta_{\mathbf{q}} d_{\mathbf{k}-\mathbf{q}\downarrow} c_{\mathbf{k}\downarrow} \rangle = \frac{2\sqrt{2}}{N} \left\langle \beta_{\mathbf{q}} \left(\sum_{i \in \uparrow} S_i^+ e^{i\mathbf{q} \cdot \mathbf{r}_i} \right) \right\rangle \\ &= \frac{2\sqrt{2}}{N} \left\langle \beta_{\mathbf{q}} \left(\sum_{i \in \uparrow} (1 - a_i^\dagger a_i) a_i e^{i\mathbf{q} \cdot \mathbf{r}_i} \right) \right\rangle \approx \sqrt{\frac{2}{N}} v_{\mathbf{q}}. \end{aligned} \quad (25)$$

There is some ambiguity in the last step of this derivation. If we neglect quartic term $\beta_{\mathbf{q}}(1 - a_i^\dagger a_i) a_i \rightarrow \beta_{\mathbf{q}} a_i$, we get a value of $b_{\mathbf{k}, \mathbf{q}}$ by a factor of $\sqrt{2}$ larger than that given by Eq. (25). If we treat the quartic term on the mean-field level, then $a_i^\dagger a_i \rightarrow 1/2$ and we get a value of $b_{\mathbf{k}, \mathbf{q}}$, a factor of $\sqrt{2}$ smaller than in Eq. (25). The correct value is somewhere in between. We choose the vertex $b_{\mathbf{k}, \mathbf{q}}$ to be the same as in the zero-temperature case.⁷ We will see that this provides the correct sum rule for the Green's function G_c , and this is a justification of our choice. We stress that Eq. (25) is a bare vertex. It corresponds to the instantaneous creation of a hole+spin wave, but not the creation of a hole with a subsequent decay into a hole+spin wave.

A. Finite-temperature correction for G_c

At finite temperature there is another possibility: the creation of a hole with the absorption of a spin wave from the thermal bath. We denote this amplitude by $c_{\mathbf{k}, \mathbf{q}}$. It is shown in Fig. 3(c), and for simplicity we also denote it as a circled cross. The derivation of $c_{\mathbf{k}, \mathbf{q}}$ is quite similar to Eq. (25) and the result is

$$c_{\mathbf{k}, \mathbf{q}} = \langle \alpha_{-\mathbf{q}}^\dagger d_{\mathbf{k}-\mathbf{q}\downarrow} c_{\mathbf{k}\downarrow} \rangle \approx \sqrt{\frac{2}{N}} u_{\mathbf{q}}. \quad (26)$$

In Eqs. (25) and (26) we have omitted the standard Bose statistics factors, $\sqrt{1+n_{\mathbf{q}}}$ in Eq. (25) and $\sqrt{n_{\mathbf{q}}}$ in Eq. (26). These factors are taken into account separately in the calculation of the diagrams.

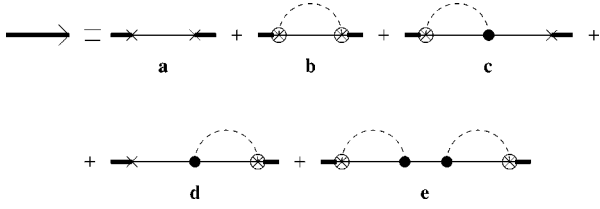


FIG. 4. Dyson equation relating Green's functions G_c (thick solid line) and G_d (thin solid line).

Now we can find the relation between the Green's functions G_c , Eq. (23), and G_d , Eq. (5). In leading t approximation it is given by the diagrams presented in Fig. 4 where the thin solid line represents the bare hole Green's function G_{0d} , Eq. (7). Each self-energy insertion should be understood as a combination of spin-wave emission and spin-wave absorption diagrams, similar to that in Fig. 1. Now let us dress these diagrams by higher orders in the hopping t . As we already discussed above, there is no single-loop correction to the "dot." We neglect double-loop corrections to the "dot" as it has been done in the SCBA. Therefore the only possibility is the introduction of self-energy corrections to G_d . To take into account all these corrections we need just to replace all bare hole Green's functions G_{0d} by dressed hole Green's functions G_d .

So Fig. 4 actually represents a Dyson equation relating G_c , Eq. (23), and G_d , Eq. (5). In analytical form it is

$$G_c(\epsilon, \mathbf{k}) = a_{\mathbf{k}}^2 G_d(\epsilon, \mathbf{k}) + \Sigma_1(\epsilon, \mathbf{k}) + 2a_{\mathbf{k}} G_d(\epsilon, \mathbf{k}) \Sigma_2(\epsilon, \mathbf{k}) + G_d(\epsilon, \mathbf{k}) \Sigma_2^2(\epsilon, \mathbf{k}), \quad (27)$$

where

$$\Sigma_1(\epsilon, \mathbf{k}) = \sum_{\mathbf{q}} [(1+n_{\mathbf{q}}) b_{\mathbf{k}-\mathbf{q}, \mathbf{q}}^2 G_d(\epsilon - \omega_{\mathbf{q}}, \mathbf{k} - \mathbf{q}) + n_{\mathbf{q}} c_{\mathbf{k}, \mathbf{q}}^2 G_d(\epsilon + \omega_{\mathbf{q}}, \mathbf{k} + \mathbf{q})] \quad (28)$$

and

$$\Sigma_2(\epsilon, \mathbf{k}) = \sum_{\mathbf{q}} [(1+n_{\mathbf{q}}) b_{\mathbf{k}-\mathbf{q}, \mathbf{q}} g_{\mathbf{k}-\mathbf{q}, \mathbf{q}} G_d(\epsilon - \omega_{\mathbf{q}}, \mathbf{k} - \mathbf{q}) + n_{\mathbf{q}} c_{\mathbf{k}, \mathbf{q}} g_{\mathbf{k}, \mathbf{q}} G_d(\epsilon + \omega_{\mathbf{q}}, \mathbf{k} + \mathbf{q})]. \quad (29)$$

B. Sum rules

Let us check now the sum rules. All singularities of retarded Green's functions are in the lower half plane of complex ϵ . Therefore, if we integrate Eq. (19) over ϵ from $-\infty$ to $+\infty$, this integral can be replaced by the integral over an infinite semicircle in the upper ϵ half plane. For infinite ϵ , $G_d = G_{0d}$, and we get the well-known sum rule

$$-\frac{1}{\pi} \text{Im} \int_{-\infty}^{\infty} G_d(\epsilon, \mathbf{k}) d\epsilon = 1, \quad (30)$$

which agrees with Eq. (4). If we integrate Eq. (27) in the same limits, the terms which contain more than one Green's function give no contribution, because the integral can be transferred into the upper complex ϵ half plane, and we find

$$\begin{aligned} & -\frac{1}{\pi} \text{Im} \int_{-\infty}^{\infty} G_c(\epsilon, \mathbf{k}) d\epsilon \\ &= \left(-\frac{1}{\pi} \text{Im} \int G_d(\epsilon, \mathbf{k}) d\epsilon \right) \\ & \times \left(a_{\mathbf{k}}^2 + \sum_{\mathbf{q}} [(1+n_{\mathbf{q}}) b_{\mathbf{k}-\mathbf{q}, \mathbf{q}}^2 + n_{\mathbf{q}} c_{\mathbf{k}, \mathbf{q}}^2] \right) \\ &= 0.5 + \frac{2}{N} \sum_{\mathbf{q}} [(1+n_{\mathbf{q}}) v_{\mathbf{q}}^2 + n_{\mathbf{q}} u_{\mathbf{q}}^2] \\ &= \frac{2}{N} \sum_{\mathbf{q}} \frac{A}{\omega_{\nu \mathbf{q}}} (1 + 2n_{\mathbf{q}}) = 1, \end{aligned} \quad (31)$$

where we have used Eqs. (13) and (15). Thus Eq. (27) reproduces the correct normalization: $\langle 0 | c_{\mathbf{k}\uparrow}^\dagger c_{\mathbf{k}\uparrow} | 0 \rangle = 1$. This also proves that the vertices (25) and (26) are correct.

The vertices $b_{\mathbf{k}, \mathbf{q}}$, Eq. (25), and $c_{\mathbf{k}, \mathbf{q}}$, Eq. (26), are invariant under translation by the inverse vector of magnetic sublattice $\mathbf{Q} = (\pm\pi, \pm\pi)$: $b_{\mathbf{k}+\mathbf{Q}, \mathbf{q}} = b_{\mathbf{k}, \mathbf{q}}$. At the same time the vertex $g_{\mathbf{k}, \mathbf{q}}$, Eq. (17), changes sign under this translation: $g_{\mathbf{k}+\mathbf{Q}, \mathbf{q}} = -g_{\mathbf{k}, \mathbf{q}}$. Therefore the self-energy $\Sigma_2(\epsilon, \mathbf{k})$ changes sign at $\mathbf{k} \rightarrow \mathbf{k} + \mathbf{Q}$ and

$$G_c(\epsilon, \mathbf{k} + \mathbf{Q}) \neq G_c(\epsilon, \mathbf{k}). \quad (32)$$

The imaginary part of $G_c(\epsilon, \mathbf{k})$ gives directly the spectra measured in ARPES experiments. This Green's function can be calculated using the Dyson equation (27) as soon as we have found G_d in the SCBA, Eq. (19).

C. Results for G_c

Numerical evaluation of G_c at finite temperature, however, is more complicated than at $T=0$. The problem lies in the infrared divergence of the integrand of $\Sigma_1(\epsilon, \mathbf{k})$ at small \mathbf{q} . To clarify this we compare the small- q behavior of the integrands of the self-energies Σ , Σ_1 , and Σ_2 . Small q means that $1/\xi_M \ll q \ll T$, where $\xi_M \propto \exp(1.1/T)$ is the magnetic correlation length. In this region the spin-wave mean occupation number is $n_{\mathbf{q}} \sim T/q$, and the vertices are $g_{\mathbf{k}, \mathbf{q}} \sim \sqrt{q}$, $b_{\mathbf{k}, \mathbf{q}} \approx c_{\mathbf{k}, \mathbf{q}} \sim 1/\sqrt{q}$. The self-energy Σ has an integrand $\propto n_{\mathbf{q}} g_{\mathbf{k}, \mathbf{q}}^2 d^2 q \sim T q d q$. It is convergent at small q and therefore numerical calculation of Σ is straightforward and the finite-temperature generalization of the SCBA is as simple as zero-temperature SCBA. For the integrand of the self-energy Σ_2 one finds $\propto n_{\mathbf{q}} b_{\mathbf{k}, \mathbf{q}} g_{\mathbf{k}, \mathbf{q}} d^2 q \sim T d q$, which is also convergent at small q . The situation is different in the self-energy Σ_1 : It is logarithmically divergent at small q : $\propto n_{\mathbf{q}} b_{\mathbf{k}, \mathbf{q}}^2 d^2 q \sim T d q / q$. There is no real divergence, however, because the integral is convergent at $q \sim 1/\xi_M$, but to calculate this integral numerically by "crude force" one needs a grid with $\Delta q \ll 1/\xi_M$. One then needs, for example, when $T=0.25$, a lattice of at least 200×200 , and for lower temperatures an even bigger lattice.

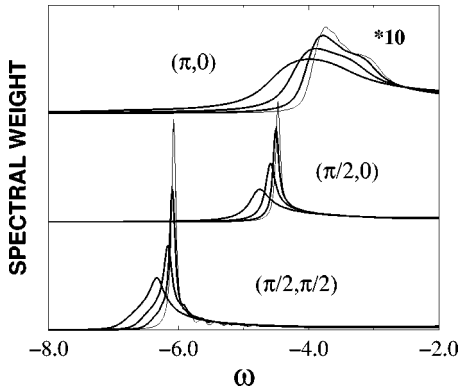


FIG. 5. Plots of $(-1/\pi)\text{Im}G_c(\omega, \mathbf{k})$ for different temperatures and \mathbf{k} points. The thin line is the result for $T=0.01$, the thick lines for $T=0.2, 0.3$, and 0.4 . The spectral weight at the $(\pi, 0)$ point is multiplied by a factor of 10.

We can avoid this problem by renormalizing Σ_1 , so that we can work with a reasonable grid size. Let us rewrite Eq. (28) in the form

$$\Sigma_1(\epsilon, \mathbf{k}) = \Sigma_R(\epsilon, \mathbf{k}) + \Sigma_{RR}(\epsilon, \mathbf{k}), \quad (33)$$

where

$$\begin{aligned} \Sigma_R(\epsilon, \mathbf{k}) = & \sum_{\mathbf{q}} (1 + n_{\mathbf{q}}) b_{\mathbf{k}-\mathbf{q}, \mathbf{q}}^2 [G_d(\epsilon - \omega_{\mathbf{q}}, \mathbf{k} - \mathbf{q}) - G_d(\epsilon, \mathbf{k})] \\ & + \sum_{\mathbf{q}} n_{\mathbf{q}} c_{\mathbf{k}, \mathbf{q}}^2 [G_d(\epsilon + \omega_{\mathbf{q}}, \mathbf{k} + \mathbf{q}) - G_d(\epsilon, \mathbf{k})] \end{aligned} \quad (34)$$

and

$$\Sigma_{RR}(\epsilon, \mathbf{k}) = G_d(\epsilon, \mathbf{k}) \sum_{\mathbf{q}} [(1 + n_{\mathbf{q}}) b_{\mathbf{k}-\mathbf{q}, \mathbf{q}}^2 + n_{\mathbf{q}} c_{\mathbf{k}, \mathbf{q}}^2]. \quad (35)$$

Numerical calculation of Σ_R does not cause any trouble because it is well convergent at small q . On the other hand, Σ_{RR} can be easily calculated analytically using the modified spin-wave theory equations (13) and (15): $\Sigma_{RR}(\epsilon, \mathbf{k}) = \frac{1}{2} G_d(\epsilon, \mathbf{k})$. Using this procedure the calculation can be done at arbitrary small temperature. The results are practically independent of the grid as soon as it is larger than 20×20 . The plots of $(-1/\pi)\text{Im}G_c(\epsilon, \mathbf{k})$ as a function of ϵ for $\mathbf{k} = (\pi/2, \pi/2)$, $\mathbf{k} = (\pi/2, 0)$, and $\mathbf{k} = (\pi, 0)$ are presented in Fig. 5.

The half widths of quasiparticle peaks of G_c are slightly larger than the half widths of quasiparticle peaks of G_d . The

spectra at $T=0.01$ agrees quite well with zero-temperature calculations.⁷ We stress that the agreement is not trivial. At $T=0$ long-range antiferromagnetic order is assumed, and in the present work we used a quite different approach based on a state without long-range order. The agreement indicates that these two approaches are consistent. For nonzero temperatures the trend in the spectra for G_c is the same as for G_d ; the temperature effect is to shift the quasiparticle peaks uniformly to lower energies and to broaden them. The spectra presented in Fig. 5 should be directly compared with ARPES experimental data.^{1,2} They reasonably reproduce positions and residues of experimental peaks, but fail to reproduce widths of the peaks.

IV. CONCLUSIONS

We considered the two-dimensional t - t' - t'' - J model at finite temperature, and developed a technique to deal with the state without long-range antiferromagnetic order. There is hope to extend this technique to the quantum-disordered state of the doped system. We generalized the self-consistent Born approximation to the case of nonzero temperature and derived the Dyson equation which relates the single-hole Green's function with fixed spin to the single-hole Green's function with fixed pseudospin. This equation is sensitive to very large distances of the order of the magnetic correlation length and therefore not convenient for computations. To overcome this problem we developed a renormalization procedure which allows one to exclude large distances and to work with a relatively small lattice: The results are independent of the lattice size as soon as it is larger than 20×20 . The effect of a finite temperature is a broadening and a shift of the quasiparticle peaks to lower energy, independent of the momentum. This is attributed to the frustrated magnetic order at finite temperature. The calculated ARPES spectra demonstrate that temperature broadening is not enough to explain the widths of the experimental spectra.^{1,2} This strengthens the argument that other degrees of freedom contribute to the peak width.⁷

ACKNOWLEDGMENTS

We are very grateful to M. Kuchiev and G.A. Sawatzky for stimulating discussions. This work was financially supported by the Nederlandse Stichting voor Fundamenteel Onderzoek der Materie (FOM) and the Stichting Scheikundig Onderzoek Nederland (SON), both financially supported by the Nederlandse Organisatie voor Wetenschappelijk Onderzoek (NWO).

*Permanent address: Materials Science Center, University of Groningen, Nijenborgh 4, 9747 AG Groningen, The Netherlands.

[†]Also at the Budker Institute of Nuclear Physics, 630090 Novosibirsk, Russia.

¹B. O. Wells *et al.*, Phys. Rev. Lett. **74**, 964 (1995).

²J. J. Pothuisen *et al.*, Phys. Rev. Lett. **78**, 717 (1997).

³S. LaRosa *et al.*, Phys. Rev. B **56**, R525 (1997).

⁴A. Nazarenko, K. J. E. Vos, S. Haas, E. Dagotto, and R. J. Gooding, Phys. Rev. B **51**, 8676 (1995).

⁵J. Bala, A. M. Oles, and J. Zaanen, Phys. Rev. B **52**, 4597 (1995).

⁶O. K. Andersen *et al.*, J. Phys. Chem. Solids **56**, 1573 (1995).

⁷O. P. Sushkov, G. Sawatzky, R. Eder, and H. Eskes, Phys. Rev. B **56**, 11 769 (1997).

⁸M. Takahashi, Phys. Rev. B **40**, 2494 (1989).

⁹Y. Tokura *et al.*, Phys. Rev. B **41**, 11 657 (1990).

¹⁰M. Greven *et al.*, Phys. Rev. Lett. **72**, 1096 (1994).

¹¹S. Schmitt-Rink, C. M. Varma, and A. E. Ruckenstein, Phys. Rev. Lett. **60**, 2793 (1988).

- ¹²C. L. Kane, P. A. Lee, and N. Read, Phys. Rev. B **39**, 6880 (1989).
- ¹³G. Martinez and P. Horsch, Phys. Rev. B **44**, 317 (1991).
- ¹⁴Z. Liu and E. Manousakis, Phys. Rev. B **45**, 2425 (1992).
- ¹⁵O. P. Sushkov, Phys. Rev. B **49**, 1250 (1994).
- ¹⁶E. Manousakis, Rev. Mod. Phys. **63**, 1 (1991).
- ¹⁷F. J. Dyson, Phys. Rev. **102**, 1217 (1956); **102**, 1230 (1956); S. V. Maleev, Zh. Éksp. Teor. Fiz. **30**, 1010 (1957) [Sov. Phys. JETP **6**, 776 (1958)].
- ¹⁸R. Eder, Y. Ohta, and G. Sawatzky, Phys. Rev. B **55**, R3414 (1997).